J. Phys. B: At. Mol. Opt. Phys. **41** (2008) 015204 (6pp) doi:10.1088/0953-4075/41/1/015204

# Modified two-centre continuum wavefunction: application to the dissociative double ionization of $H_2$ by electron impact

**O Chuluunbaatar[1], B B Joulakian[2], I V Puzynin[1], Kh Tsookhuu[3] and S I Vinitsky[1]**

[1] Joint Institute for Nuclear Research, Dubna, Moscow Region 141980, Russia
[2] Université Paul Verlaine—Metz, Laboratoire de Physique Moléculaire et des Collisions, 1 Bd Arago, 57078 Metz Cedex 3, France
[3] National University of Mongolia, School of Physics and Electronics, Ulaanbaatar, Mongolia

Received 25 July 2007, in final form 29 October 2007
Published 19 December 2007
Online at stacks.iop.org/JPhysB/41/015204

**Abstract**
The fully differential cross section (FDCS) of the double ionization of the hydrogen molecule by electron impact, with the coincidence detection of the two ejected and the scattered electrons, is determined by the application of a product of two modified two-centre Coulomb continuum (MTCC) wavefunctions describing the two ejected electrons. The MTCC, which fulfils the correct boundary conditions asymptotically up to the order $O((kr)^{-2})$, is obtained in a closed analytical form by solving the Schrödinger equation of an electron with wave vector **k** and position vector **r** in the Coulomb field of two fixed nuclei. After the study of the variation of the (FDCS) for some typical geometries the multiply differential cross section of the (e, 3 − 1e) process is determined and compared to the experimental values.

## 1. Introduction

The multiple ionization of atoms and molecules by photon or charged-particle impact is of considerable interest in many branches of physics, such as plasma physics, astrophysics and radio-physics, as it results in the transfer of an appreciable amount of energy to the target and consequently to its environment. Such processes are also important to understand the electronic structure, the ionization mechanisms and to probe electron–electron correlation in the case of double ionization which is the main cause of this process [1].

The coincidence detection techniques, measuring the momenta of fragments emerging from atomic collision processes and especially from dissociative ionization experiments of diatomic species by electron impact, are now undergoing a very rapid development [2–5]. This type of coincidence detections has been already performed in collision experiments involving the multiply charged ionic projectiles and the hydrogen molecule [6–9].

The electronic two-centre problem, met in the study of inelastic collisions of diatomic targets, is very closely related to the Coulomb three-body problem that one meets in simple ionization experiments by electron impact [10]. In the last few years, many elegant models have been proposed to describe the dynamics of the ejected electron in an (e, 2e) experiment, which presents a unique physical situation together with that of ($\gamma$, e), where an electron can be found in the field of two fixed nuclei. Joulakian *et al* [11] used an approximate 3C-type one parameter wavefunction inspired from the Pluvinage model [12] constructed by the product of two Coulomb functions. Serov *et al* [13] compared a wave packet evolution approach to that using partial waves constructed by the exact solutions in prolate spheroidal coordinates of the two-centre Coulomb problem [14].

In this paper, we study theoretically the double ionization of $H_2$ by electron impact by describing the double electronic two-centre continuum by a product of two modified two-centre Coulomb continuum (MTCC) [15] wavefunctions. This is particularly interesting, as the double continuum is

 

constituted by two equivalent electrons coming from the electron cloud of the same target, in contrast to (e, 2e) experiments, where only one of the electrons comes from the target. This permits the verification of different theoretical models proposed to describe the electronic continuum and understand the mechanisms of the double ionization. Up to now, (e, 3e) experiments have only been performed on atoms [16]. Recently, (e, 3 − 1e) experiments on molecular hydrogen at about 600 eV incident energy have been reported [17]. These experiments are double ionization experiments, where only one of the ejected electrons is detected in coincidence with the scattered electron.

The paper is organized as follows. In section 2, we give briefly the basic expressions to calculate the fully differential ionization dissociation cross section of the ground state of a hydrogen molecule ion by a fast electron. In section 3, we present and comment on our results, and conclude.

## 2. Theory

The differential cross section, in a general out-of-plane geometry of the three electrons and one of the protons $H^+$ is nine fold and it is given by

$$\sigma^{(9)} = \frac{\mathrm{d}^9\sigma}{\mathrm{d}\Omega_\rho\,\mathrm{d}\theta_s\,\mathrm{d}\Omega_1\,\mathrm{d}\Omega_2\,\mathrm{d}\left(k_1^2/2\right)\mathrm{d}\left(k_2^2/2\right)} = \frac{k_1k_2k_s}{k_i}|T_{fi}|^2, \tag{1}$$

where $\Omega_\rho$, $\Omega_1$ and $\Omega_2$ are the solid angles of the internuclear axis and the ejection directions. Here, the directions of the incident and the scattered electrons define the reference plane such that for the scattered electron we need only the polar angle $\theta_s$. $k_i, k_s, k_1$ and $k_2$ represent respectively the moduli of the wave vectors of the incident, scattered and ejected electrons. Assuming that all directions of the molecule are equally probable, we average over all the possible directions of the internuclear axis to obtain the seven-fold differential cross section:

$$\sigma^{(7)} = \frac{1}{4\pi}\int \mathrm{d}\Omega_\rho\sigma^{(9)}. \tag{2}$$

The conservation of the energy for fixed internuclear distance $\rho$ gives

$$E_i = E_s + E_1 + E_2 + I, \tag{3}$$

where $E_i$, $E_s$, $E_1$ and $E_2$ represent respectively the energies of the incident, scattered and ejected electrons, $I = 51$ eV being the energy necessary to eject two electrons from the target at the equilibrium internuclear distance $\rho_e = 1.4$ au. In the frame of first-order Born approximation, ignoring exchange between the incident and the ejected electrons, the transition matrix element $T_{fi}$ will be given in the case of an unpolarized incident electron beam by

$$T_{fi} = \frac{1}{2\pi}\int \mathrm{d}\mathbf{r}_1\int \mathrm{d}\mathbf{r}_2\int \mathrm{d}\mathbf{R}\,\exp(\imath\mathbf{K}\mathbf{R})\chi_f^*(\mathbf{r}_1,\mathbf{r}_2) \times V\vartheta_{\Sigma_g}(r_1,r_2,\rho), \tag{4}$$

where $\mathbf{r}_j$ $(j = 1, 2)$ refer to the positions of the bound electrons, $\chi_f^*$ represents the complex conjugate of the wavefunction describing the two ejected electrons, $\mathbf{R}$ represents the position of the fast incident electron described here by a plane wave and $\mathbf{K} = \mathbf{k}_i - \mathbf{k}_s$ gives the momentum transferred to the target. The potential $V$ represents the interaction between the incident electron and the target $H_2$

$$V = -\frac{Z}{R_a} - \frac{Z}{R_b} + \frac{1}{r_{1p}} + \frac{1}{r_{2p}} \tag{5}$$

with $Z = 1$ for $H_2$. From figure 1 we can have

$$\begin{aligned} \mathbf{R}_a &= \mathbf{R} + \boldsymbol{\rho}/2, & \mathbf{r}_{1p} &= \mathbf{R} - \mathbf{r}_1,\\ \mathbf{r}_{1a} &= \mathbf{r}_1 + \boldsymbol{\rho}/2, & \mathbf{r}_{2a} &= \mathbf{r}_2 + \boldsymbol{\rho}/2,\\ \mathbf{R}_b &= \mathbf{R} - \boldsymbol{\rho}/2, & \mathbf{r}_{2p} &= \mathbf{R} - \mathbf{r}_2,\\ \mathbf{r}_{1b} &= \mathbf{r}_1 - \boldsymbol{\rho}/2, & \mathbf{r}_{2b} &= \mathbf{r}_2 - \boldsymbol{\rho}/2, \end{aligned} \tag{6}$$

where $R_a$, $R_b$ and $r_{ja}, r_{jb}$ are the distances of the incident electron and ejected electron $j$ from the nuclei $a$ and $b$, respectively; $r_{jp}$ is the distance of the incident electron from the ejected electron $j$. The wavefunction $\vartheta_{\Sigma_g}(r_1, r_2, \rho)$ describes the initial electronic $\Sigma_g$ fundamental state of the target and was obtained by a variational three-parameter calculation borrowed from [18]

$$\vartheta_{\Sigma_g}(r_1,r_2,\rho) = N(\rho)(\phi(1)\psi(2) + \psi(1)\phi(2)), \tag{7}$$

with

$$\begin{aligned} \phi(j) &= x_a(j) + \epsilon x_b(j), & \psi(j) &= \epsilon x_a(j) + x_b(j),\\ x_a(j) &= \exp(-\beta\xi_j - \gamma\eta_j), & x_b(j) &= \exp(-\beta\xi_j + \gamma\eta_j), \end{aligned} \tag{8}$$

where $\xi_j = (r_{ja} + r_{jb})/\rho$, $\eta_j = (r_{ja} - r_{jb})/\rho$; $\beta = 0.835$, $\gamma = 0.775$ and $\epsilon = 0.137$ are variational parameters that we have determined for the equilibrium internuclear distance $\rho_e = 1.4$ au. Here the norm $N(\rho_e) = 0.255$ and the ground-state energy is equal to $-1.149$ au.

In the final state, the two ejected electrons in the field of the two nuclei will be described by a product of two MTCC [15]:

$$\chi_f(\mathbf{r}_1,\mathbf{r}_2) = \upsilon(|\mathbf{k}_1 - \mathbf{k}_2|) \times \frac{\phi_f(\mathbf{k}_1,1)\phi_f(\mathbf{k}_2,2) + \phi_f(\mathbf{k}_2,1)\phi_f(\mathbf{k}_1,2)}{\sqrt{2}}, \tag{9}$$

with

$$\phi_f(\mathbf{k}_i,j) = M_i\frac{\exp(\imath\mathbf{k}_i\mathbf{r}_j)}{(2\pi)^{3/2}}\prod_{\gamma=a}^{b}{}_1F_1 \times\left(\imath\alpha_i, 1-\imath\varepsilon_i, -\imath\left[k_ir_{j_\gamma} + \mathbf{k}_i\mathbf{r}_{j_\gamma}\right]\right), \tag{10}$$

$$M_i = \exp(-\pi\alpha_i)\frac{\Gamma(1-\imath\alpha_i-\imath\varepsilon_i)^2}{\Gamma(1-\imath\varepsilon_i)^2}, \tag{11}$$

where ${}_1F_1(a, b, x)$ is the Kummer confluent hypergeometric function, $\alpha_i = -Z/k_i$ is the Sommerfeld parameter and $\varepsilon_i$ is the small real parameter. The term $\upsilon$ is the repulsive Gamow factor:

$$\begin{aligned} \upsilon(|\mathbf{k}_1 - \mathbf{k}_2|) &= \exp(-\pi\alpha_{12}/2)\Gamma(1-\imath\alpha_{12}),\\ \alpha_{12} &= \frac{1}{|\mathbf{k}_1 - \mathbf{k}_2|}. \end{aligned} \tag{12}$$

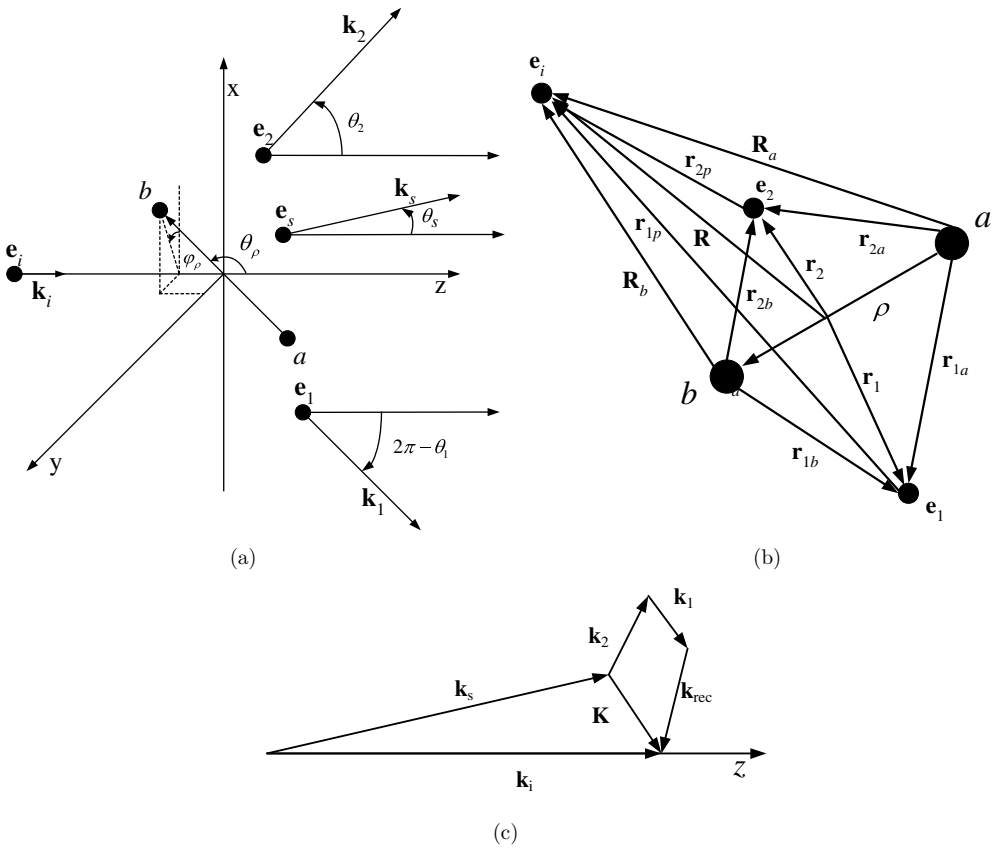


**Figure 1.** (a) The reference frame with the different wave vectors $\mathbf{k}_i$, $\mathbf{k}_s$, $\mathbf{k}_1$ and $\mathbf{k}_2$ representing the momenta of the incident, scattered the two ejected electrons, respectively. $\theta_s$, $\theta_1$ and $\theta_2$ denote the scattered and ejected electron angles, respectively. (b) The different position vectors of the incident and the bound electrons with respect to the two nuclei. (c) The different wave vectors which define the momentum transfer $\mathbf{K}$ and the recoil momentum and $\mathbf{k}_{\rm rec}$ by momentum conservation law.

Integrating over the position of the fast incident electron $\mathbf{R}$ using the Bethe transformation

$$\int \frac{\mathrm{d}\mathbf{R}}{|\mathbf{R}-\mathbf{r}|}\exp(\imath\mathbf{K}\mathbf{R}) = \frac{4\pi\exp(\imath\mathbf{K}\mathbf{r})}{K^2} \tag{13}$$

and substituting the functions defined in equations (7) and (9) into equation (4), and using the Fourier transform for one of the centres for each electron, we get

$$T_{fi} = -\frac{2\sqrt{2}N(\rho)}{(2\pi)^9\mathbf{K}^2}\exp(\imath(\mathbf{K}-\mathbf{k}_1-\mathbf{k}_2)\boldsymbol{\rho}/2) \times M[(\epsilon^2+1)D+2\epsilon P], \tag{14}$$

where

$$\begin{aligned} M &= \upsilon^*(|\mathbf{k}_1-\mathbf{k}_2|)M_1^*M_2^*,\\ D &= H(\mathbf{k}_1,\mathbf{k}_2,\mathbf{K},X,Y)\\ &\quad - Z(1+\exp(-\imath\mathbf{K}\boldsymbol{\rho}))G(\mathbf{k}_1,\mathbf{k}_2,X,Y),\\ P &= U(\mathbf{k}_1,\mathbf{k}_2,\mathbf{K},X,Y)\\ &\quad - Z(1+\exp(-\imath\mathbf{K}\boldsymbol{\rho}))S(\mathbf{k}_1,\mathbf{k}_2,X,Y), \end{aligned} \tag{15}$$

with

$$\begin{aligned} &H(\mathbf{k}_1,\mathbf{k}_2,\mathbf{K},X,Y)\\ &\quad = H_1(\mathbf{k}_1,\mathbf{k}_2,\mathbf{K},X,Y)+H_2(\mathbf{k}_2,\mathbf{k}_1,\mathbf{K},X,Y),\\ &H_j(\mathbf{k}_j,\mathbf{k}_{3-j},\mathbf{K},X,Y)\\ &\quad = I(\mathbf{k}_j,\mathbf{k}_{3-j},\mathbf{K},X,Y)+I(\mathbf{k}_j,\mathbf{k}_{3-j},\mathbf{K},Y,X),\\ &G(\mathbf{k}_1,\mathbf{k}_2,X,Y)\\ &\quad = I(\mathbf{k}_1,\mathbf{k}_2,0,X,Y)+I(\mathbf{k}_1,\mathbf{k}_2,0,Y,X),\\ &U(\mathbf{k}_1,\mathbf{k}_2,\mathbf{K},X,Y)\\ &\quad = U_1(\mathbf{k}_1,\mathbf{k}_2,\mathbf{K},X,Y)+U_2(\mathbf{k}_2,\mathbf{k}_1,\mathbf{K},X,Y),\\ &U_j(\mathbf{k}_j,\mathbf{k}_{3-j},\mathbf{K},X,Y)\\ &\quad = J(\mathbf{k}_j,\mathbf{k}_{3-j},\mathbf{K},X,Y)+J(\mathbf{k}_j,\mathbf{k}_{3-j},\mathbf{K},Y,X),\\ &S(\mathbf{k}_1,\mathbf{k}_2,X,Y)\\ &\quad = J(\mathbf{k}_1,\mathbf{k}_2,0,X,Y)+J(\mathbf{k}_1,\mathbf{k}_2,0,Y,X), \end{aligned} \tag{16}$$

and

$$\begin{aligned} &I(\mathbf{k}_j,\mathbf{k}_{3-j},\mathbf{Q},X,Y)\\ &\quad = F(\mathbf{k}_j,\mathbf{k}_j-\mathbf{Q},X,Y)F(\mathbf{k}_{3-j},\mathbf{k}_{3-j},Y,X),\\ &J(\mathbf{k}_j,\mathbf{k}_{3-j},\mathbf{Q},X,Y)\\ &\quad = F(\mathbf{k}_j,\mathbf{k}_j-\mathbf{Q},X,Y)\times F(\mathbf{k}_{3-j},\mathbf{k}_{3-j},X,Y). \end{aligned} \tag{17}$$

Here $X=(\beta+\gamma)/\rho$, $Y=(\beta-\gamma)/\rho$ and

$$\begin{aligned} &F(\mathbf{k},\mathbf{q},X,Y)\\ &\quad = \int \mathbf{d}\boldsymbol{\tau}\exp(\imath\boldsymbol{\tau}\boldsymbol{\rho})W_{\alpha,\varepsilon}(\mathbf{k},\boldsymbol{\tau},X)W_{\alpha,\varepsilon}(\mathbf{k},\mathbf{q}-\boldsymbol{\tau},Y)\\ &\quad = \exp(\imath\mathbf{q}\boldsymbol{\rho})\int \mathbf{d}\boldsymbol{\tau}\exp(-\imath\boldsymbol{\tau}\boldsymbol{\rho})W_{\alpha,\varepsilon}(\mathbf{k},\boldsymbol{\tau},Y)W_{\alpha,\varepsilon}\\ &\qquad \times(\mathbf{k},\mathbf{q}-\boldsymbol{\tau},X). \end{aligned} \tag{18}$$

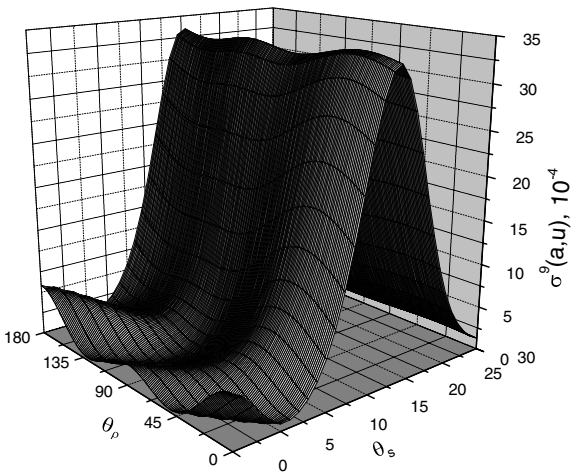


**Figure 2.** The variation of $\sigma^{(9)}$ in terms of $\theta_\rho$ and $\theta_s$ for the (e, 3e) double ionization of $H_2$ for $E_i = 612$ eV, $E_s = 500$ eV, $E_1 = 51$ eV and $E_2 = 10$ eV representing respectively the energy values of the incident, scattered and ejected electrons. The two ejected electrons emerge in opposite directions with $\mathbf{k}_1$ parallel to $\mathbf{K}$. Here $\varepsilon_1 = \varepsilon_2 = 0$.

The function $W_{\alpha,\varepsilon}(\mathbf{k}, \mathbf{q}, \lambda)$ in the integrand is given [15] by

$$W_{\alpha,\varepsilon}(\mathbf{k}, \mathbf{q}, \lambda) = \int \mathbf{dr} \exp(-\imath \mathbf{qr} - \lambda r)\, {}_1F_1(-\imath\alpha, 1 + \imath\varepsilon, \imath[kr + \mathbf{kr}])$$
$$= \frac{8\pi}{(\lambda^2 + q^2)^2}\left(\lambda\, {}_2F_1(-\imath\alpha, 2; 1 + \imath\varepsilon, x) - \frac{\alpha k}{1 + \imath\varepsilon}\, {}_2F_1(1 - \imath\alpha, 2; 2 + \imath\varepsilon, x)\right), \quad (19)$$

where $x = 2(\mathbf{qk} + \imath\lambda k)/(\lambda^2 + q^2)$ and ${}_2F_1(a, b; c, x)$ represents the hypergeometric function. For $\varepsilon = 0$ the integral in equation (19) can be evaluated analytically [11]:

$$W_{\alpha,0}(\mathbf{k}, \mathbf{q}, \lambda) = \frac{8\pi}{(\lambda^2 + q^2)^2}(1 - x)^{\imath\alpha} \times \left(\lambda(1 + \imath\alpha) - \imath\alpha\frac{\lambda - \imath k}{1 - x}\right). \quad (20)$$

## 3. Results

After verification of our procedure and testing all the symmetry properties of $\sigma^{(9)}$, we have studied its variation in terms of the orientation of the internuclear axis, the scattering and ejection angles for different values of $\varepsilon_1 = \varepsilon_2 < 1$. We have observed that the influence of the introduction of these parameters is relatively small, and does not change the structure of the curves concerning the fully differential cross section, and that it becomes sensible for the (e, 3 − 1e) results presented in figure 5. We have thus chosen to present for the next three figures only the results obtained for $\varepsilon_1 = \varepsilon_2 = 0$ for which the basic integral equation (20) can be calculated analytically. We have chosen as in the experiment of the Orsay group [17] an incident electron energy value of 612 eV. In figure 2, we show the variation of $\sigma^{(9)}$ with the orientation of the internuclear axis given by $\theta_\rho$ and the scattering angle $\theta_s$. We have chosen opposite ejection directions with $\mathbf{k}_1$ parallel to $\mathbf{K}$ and fixed ejection energy values of 51 eV and 10 eV, respectively.

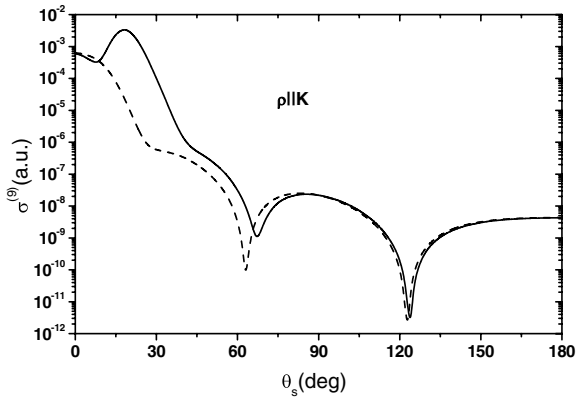


**Figure 3.** The variation of $\sigma^{(9)}$ in terms of the scattering angle $\theta_s$ of the (e, 3e) double ionization of $H_2$, for the same energy values as in figure 2. The full line corresponds to the case where $\mathbf{k}_1$ is parallel to $\mathbf{K}$ and the dashed line to the case where $\mathbf{k}_2$ is parallel to $\mathbf{K}$. Here $\varepsilon_1 = \varepsilon_2 = 0$.

It is worth noting here that, as the double ionization and dissociative ionization of $H_2$ are processes which are used to produce protons [19, 20], our present results could bring valuable information about the favourable directions for the emergence of the protons also. We of course admit here, that the electronic motion is much faster than the rotational and vibrational movements and that the ionization process is a vertical transition from the fundamental electronic level to the double continuum. In figure 2, we can observe that for small scattering angles between (0° and 5°), we have two peaks one around 170° and the other around 80°. These directions correspond respectively to situations for which the molecule is aligned with the momentum transfer and perpendicular to it. In spite of the fact that double ionization is mainly due to quantum effects such as electron–electron correlation, we can here try to explain this behaviour of $\sigma^{(9)}$ by considering the momentum conservation equation

$$\mathbf{K} = \mathbf{k}_i - \mathbf{k}_s = \mathbf{k}_1 + \mathbf{k}_2 + \mathbf{k}_{\rm rec} \quad (21)$$

where $\mathbf{k}_{\rm rec}$, the recoil momentum transferred to the target as a whole, is in this geometry parallel to $\mathbf{K}$. It is shared equally by the two nuclei, only in two situations, one when their axis is perpendicular to $\mathbf{K}$ and when they are aligned with it. Now it happens that these two situations correspond to the two maxima observed for a given $\theta_s$.

As the scattering angle is increased, we see that the two maxima follow the momentum transfer direction, until we arrive to the maximum at $\theta_s = 18°$. In this scattering direction, we can verify that the magnitude of the momentum transfer $\mathbf{K}$ has reached that of $\mathbf{k}_1$. This means that

$$\mathbf{k}_2 = -\mathbf{k}_{\rm rec} \quad (22)$$

for all values of $\theta_\rho$. This is classically the most favourable situation as for all other values of $\theta_s$, $\mathbf{k}_2$ will not be aligned to

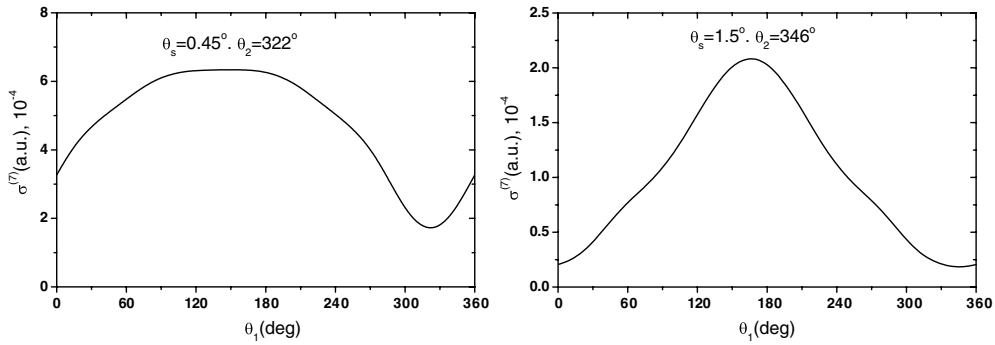


(a) (b)

**Figure 4.** The variation of $\sigma^{(7)}$ in atomic units for the (e, 3e) double ionization of $H_2$ in terms of the ejection direction of the electron 1. The ejection energy values are 51 eV and 10 eV and $\varepsilon_1 = \varepsilon_2 = 0$. (a) The incident energy value is 5612 eV with a scattering angle $\theta_s = 0.45^\circ$. (b) The incident energy value is 612 eV with a scattering angle $\theta_s = 1.5^\circ$. The ejection direction of the second electron is taken parallel to the momentum transfer **K** around $\theta_2 \simeq 330^\circ$.

$\mathbf{k}_{\rm rec}$. We also observe that $\sigma^{(9)}$ is relatively less sensitive to the variation of $\theta_\rho$ at this scattering angle. This corresponds to the Bethe ridge situation in (e, 2e) simple ionization process when $\mathbf{k_1} = \mathbf{K}$, which is a situation of a head on collision of the projectile electron with the target electron, such that the rest of the target has very little influence and does not participate in the reaction.

To show the molecular aspect in our study, we present in figure 3 the variation of $\sigma^{(9)}$ with the scattering angle for $\boldsymbol{\rho}\|\mathbf{K}$. We chose opposite ejection directions like above for two cases: in one $\mathbf{k}_1$ parallel to **K**, and second for $\mathbf{k}_2$ parallel to **K**. In both cases, interference patterns appear as expected due to the diatomic nature of the target, which plays the roll of two Young obstacles. The presence of these patterns is due to $\cos(\mathbf{K}\boldsymbol{\rho}/2)$, which appears in the expression of the transition matrix element. This is discussed in [11, 21]. In the case ($\mathbf{k}_2$ parallel to **K**) the value of $\theta_s = 15^\circ$ corresponds to the situation where the magnitude of the momentum transfer **K** is equal to the magnitude of $\mathbf{k}_2$ which is smaller. Now in this case, shown by the dashed line in figure 3, we have a much less pronounced maximum. This is due to the fact that in this case $\mathbf{k}_{\rm rec} = -\mathbf{k}_1$, which is relatively large. Now if $\mathbf{k}_{\rm rec}$ is relatively large the residual ion will get more of the available energy making the double ionization process less probable.

We next pass to the study of the variation of $\sigma^{(7)}$ obtained by equation (2). This will correspond, as we said, to experiments, where only the scattered and the ejected electrons are detected in coincidence. One high (5612 eV) and one intermediate (612 eV) incidence energy values are investigated. We have kept the ejection energy values the same as in the preceding cases. Here, we fix the ejection direction of the second electron parallel to **K** and vary the ejection angle of the first electron. This variation is shown in figures 4(a) and (b). In the case of high incidence energy, we have considered a small scattering angle $\theta_s = 0.45^\circ$ and in the case of intermediate incidence energy, a larger scattering angle $\theta_s = 1.5^\circ$. In the absence of experimental results we can observe that, as expected, opposite ejection is the most probable situation in both cases and that higher energy values give higher magnitudes for $\sigma^{(7)}$.

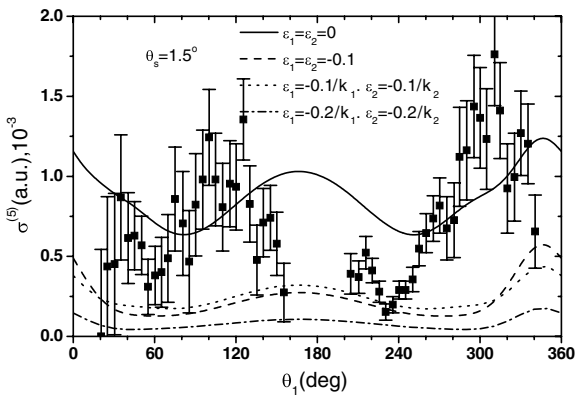


**Figure 5.** The variation of $\sigma^{(5)}$ in atomic units of the (e, 3 − 1e) double ionization of $H_2$ with the ejection angle of electron 1, for the same energy values as above as in figure 2. The unobserved electron is the one having an energy of 10 eV. The scattering angle $\theta_s = 1.5^\circ$. Full squares with error bars correspond to experimental results of [17] scaled to the theory for the best visual fit at the binary lobe (around 300°).

Once we have done, the necessary observations concerning the 'normal' behaviour of the multiply differential cross sections (MDCS) with our two-centre approach, we have tried to reproduce the results of the (e, 3 − 1e) experiments realized by the Orsay group [17]. (e, 3 − 1e) designates double ionization experiments in which the scattered and only one of the ejected electrons are detected in coincidence. The energy of the non observed electron is deduced from the energy conservation equation (3). This presents a practical advantage for the experimental realization, as it needs the coincidence detection of two electrons instead of three and thus larger MDCS. Theoretically this can be determined by integrating our results over the solid angle $\Omega_2$ of the second ejected electron

$$\sigma^{(5)} = \int {\rm d}\Omega_2 \sigma^{(7)}. \tag{23}$$

We observe in figure 5 that our method reproduces, for all the choices of $\varepsilon_i$, the experimental structure of the variation of $\sigma^{(5)}$ in terms of the ejection angle $\theta_1$, with two maxima and two minima shifted with respect to the experimental curve. The theoretical results give all the same predominant direction parallel to **K** around $\theta_1 = 350°$. The experimental curve seems to have shifted. This disagreement of theory and experiment is also observed in simple ionization (e, 2e) coincidence detection experiments, specially in the intermediate incidence energy regime. At higher incident energy values it disappear [22] and both experiment and MTCC give similar results with the predominant ejection direction parallel to **K**. Now the challenge for our theory is to explore the different improvements in the intermediate energy that we could introduce to try to match the theoretical results. We intend to introduce in a next step a diatomic distortion of the target, which will be based, by analogy to the one-centre problem, on the solutions of the two-centre Schrödinger equation separable in prolate spheroidal coordinates, which permit us to construct diatomic partial waves [14].

## 4. Conclusion

We have determined the fully differential cross section of the double ionization of $H_2$ by applying a product of two modified two-centre continuum functions. Our results show that the scattering direction, which fixes the direction of the momentum transfer, is the principal factor which will define the preferential directions for the emergence of the protons. It is also shown that as expected the two ejected electrons tend to emerge in opposite directions. The comparison with the results of (e, 3 − 1e) experiments show that the use of the first Born term in the perturbation gives the good structure, but it cannot give the optimal direction of the experiment. Here, the difficulty of describing the two-centre continuum is added to the main difficulty of describing the double electronic continuum and to the difficulty of describing second-order effects. Nevertheless, this is a preliminary work to which we intend to introduce an appropriate diatomic distorted waves constructed by the solutions of the two-centre Schrödinger equation separable in prolate spheroidal coordinates. This demands a larger-scale computational effort that we intend to realize next.

## Acknowledgments

We thank the Region of Lorraine (France) for its financial support, and the C.I.N.E.S. (Centre Informatique National de l'Enseignement Superieur) for providing computing facilities. This work was partially supported by the theme 09-6-1060-2005/2009 'Mathematical support of experimental and theoretical studies conducted by JINR'.

## References

[1] Byron F W Jr and Joachain C J 1967 *Phys. Rev.* **164** 1–9
[2] Dörner R *et al* 1996 *Phys. Rev. Lett.* **77** 1024–7
[3] Lafosse A, Houver J C and Dowek D 2001 *J. Phys. B: At. Mol. Opt. Phys.* **34** 819–37
[4] Edwards A K and Zheng Q 2001 *J. Phys. B: At. Mol. Opt. Phys.* **34** 1539–48
[5] Weber Th *et al* 2001 *J. Phys. B: At. Mol. Opt. Phys.* **34** 3669–78
[6] Corchs S E, Busnengo H F and Rivarola R D 1999 *Nucl. Instrum. Methods Phys. Res.* B **149** 247–56
[7] Wang Y D, McGuire J H and Rivarola R D 1989 *Phys. Rev.* A **40** 3673–80
[8] Corchs S E, Rivarola R D, McGuire J H and Wang Y D 1993 *Phys. Rev.* A **47** 201–207
[9] Corchs S E, Rivarola R D, McGuire J H and Wang Y D 1994 *Phys. Scr.* **50** 469–72
[10] Brauner M, Briggs J S and Klar H 1989 *J. Phys. B: At. Mol. Opt. Phys.* **22** 2265
[11] Joulakian B, Hanssen J, Rivarola R and Motassim A 1996 *Phys. Rev.* A **54** 1473–79
[12] Pluvinage P 1951 *Phys. Radium* **12** 789–92
[13] Serov V V, Derbov V L, Joulakian B B and Vinitsky S I 2001 *Phys. Rev.* A **63** 062711-1–8
[14] Serov V V, Joulakian B B, Pavlov D V, Puzynin I V and Vinitsky S I 2002 *Phys. Rev.* A **65** 062708-1–7
[15] Chuluunbaatar O, Joulakian B B, Tsookhuu Kh and Vinitsky S I 2004 *J. Phys. B: At. Mol. Opt. Phys.* **37** 2607–16
[16] Berakdar J, Lahmam-Bennani A and Dal Cappello C 2003 *Phys. Rep.* **374** 91–164
[17] Lahmam-Bennani A, Duguet A and Roussin S 2002 *J. Phys. B: At. Mol. Opt. Phys.* **35** L59–63
[18] Mueller C and Eyring H 1951 *J. Chem. Phys.* **19** 1495–7
[19] Dunn G H and Kieffer L J 1963 *Phys. Rev.* **132** 2109–2117
[20] Crowe A and McConkey J W 1973 *J. Phys. B: At. Mol. Opt. Phys.* **6** 2088–106
[21] Stolterfoht N *et al* 2001 *Phys. Rev. Lett.* **87** 023201
[22] Weck P F, Fojón O A, Joulakian B, Stia C R, Hanssen J and Rivarola R D 2002 *Phys. Rev.* A **66** 012711-1–8